PCCP

Cite this: *Phys. Chem. Chem. Phys.*, 2012, **14**, 4155–4161

www.rsc.org/pccp

PAPER

Design of amphoteric mixed oxides of zinc and Group 3 elements (Al, Ga, In): migration effects on basic features

Adrien Mekki-Berrada, Didier Grondin, Simona Bennici and Aline Auroux*

Received 16th November 2011, Accepted 27th January 2012
DOI: 10.1039/c2cp23613c

The design of new amphoteric catalysts is of great interest for several industrial processes, especially those covering dehydration and dehydrogenation phenomena. Adsorption microcalorimetry was used to monitor the design of mixed oxides of zinc with Group 3 elements (aluminium, gallium, indium) with amphoteric character and enhanced specific surface area. Acid–base features were found to evolve non-linearly with the relative amounts of metal, and the strengths of the created acidic or basic sites were measured by adsorption microcalorimetry. A panel of bifunctional catalysts of various acid–base (amounts, strengths) and redox character was obtained. Besides, special interest was given to In–Zn mixed oxides for their enhanced basicity: this series of catalysts displays important basic features of high strength (q_{diff} (SO_2 ads.) $>$ 200 kJ $mol^{-1}_{SO_2}$) in substantial amounts (1 – 2 μmol $m^{-2}_{catalyst}$), whose impact on efficiency or selectivity in catalytic dehydration/dehydrogenation can be valuable.

Introduction

Solids possessing both acidic and basic features usually display an interesting catalytic activity for dehydration or dehydrogenation, of common use in industrial processes (polymers, biofuels and additives).[1] Such is the case of zinc oxide and the oxides from Group 3 (Al, Ga, In), which display both sites in similar amounts on their surface and can be called amphoteric. The competition between dehydration and dehydrogenation properties of an amphoteric catalyst is usually influenced by its relative acidic and basic features. In the case of zinc oxide, Lewis and Brønsted acid sites were found to enhance acetamide dehydration activity in propan-2-ol decomposition.[2] A study on the oxides of Group 3 elements supported on niobium oxide has already been carried out by Petre *et al.*, comparing microcalorimetric results with catalytic activity in the dehydrogenation of propane to propene reaction. The supported catalysts' activity was growing with decreasing acidity, but the ratio of acidic to basic sites and the homogeneity (dispersion) were found as the main criteria for determining the activity.[3] Microcalorimetry studies have been widely carried out on bulk oxides and molecular sieves, with the intent of obtaining a better understanding of the acidity and basicity of solids, and several reviews and tables can be found,[4–7] however the acid–base features can vary with the preparation of the solid, and mixed oxides can display original features, non-linear to the bulk oxides they stem from. Microcalorimetry studies are then very appropriate to characterize these catalysts, such as gallia–alumina synthesized by Gergely *et al.* by impregnation of gallium nitrate on alumina with variable relative amounts, for which similar acid–base features were obtained for the whole series, with a slightly enhanced basic strength with increasing gallium loading.[8] A microcalorimetric study of In_2O_3/Al_2O_3 catalysts of variable indium oxide loading on alumina confirmed the correlation between balanced acidic and redox properties and good efficiency in the catalytic $DeNO_x$ activity.[9] Zinc oxide has been vastly studied for its physical properties when doped (*n*-doping with Group 3 metal elements such as In, Al or Ga), its use as a heterogeneous photocatalyst,[10] as a sensor for CO_x, NO_x or SO_2,[11] or as a nanosize material for efficient catalytic water gas shift reaction and methanol synthesis.[12] However most studies on ZnO focused on nanosized material for which acid–base considerations are off-topic, or more generally did not provide a thorough acid–base study on such amphoteric oxide powders. Commercial zinc oxide is most often obtained by sublimation of zinc powder at 1300–1700 K in an air flow followed by its direct oxidation and deposition as zinc oxide (indirect "French" process); its crystallinity is high but its specific surface area is very low (5 m^2 g^{-1}).[13] The lower temperature syntheses and the mixing or supporting of zinc oxide on other oxides can improve its specific surface area, which is advantageous for a heterogeneous catalyst. In this article, in order to design new series of amphoteric catalysts, mixed oxides were synthesized *via* a process adapted from Naik and Fernandes,[2,14] while the evolution of their acid–base features was monitored by adsorption microcalorimetry. Deriving the total number of acidic and basic sites and their corresponding strengths, and associating it with

IRCELYON, CNRS UMR5256, Université Lyon1, 2 avenue Albert Einstein, Villeurbanne, France. E-mail: aline.auroux@ircelyon.univ-lyon1.fr; Fax: +33-(0)472-44-53-99; Tel: +33-(0)472-44-53-98

characterization by XRD and XPS analyses brought more understanding on the nature of these new amphoteric oxides. Besides, their redox character was determined by TPR and allowed us to assess the bifunctionality of the samples.

Experimental methods

The pure (ZnO, Ga_2O_3, Al_2O_3, In_2O_3) and mixed oxides (Ga–Zn, Al–Zn, In–Zn) were prepared following a process adapted from a work by Naik and Fernandes,[2,14] by heating intimate mixtures of metal nitrates, oxalic acid and urea in air (50 mL min^{-1}) at 653 K for 7 h. During the synthesis process, the mixing of both nitrates resulted in desorption of water from the salts leading to a cream-like precursor. Table 1 gathers molar ratios of the precursors of prepared oxides and the effective metal amounts (relative molar ratios $X:100-X$) as measured by chemical analysis (ICP-OES "Activa" Jobin Yvon). Commercial zinc oxide (De Craene), γ-alumina (DEGUSSA), gallium oxide (STREM) and indium oxide (STREM) were used for comparison with synthesized bulk oxides.

The specific surface area (BET) was determined by nitrogen adsorption at 77 K on an ASAP 2020 (Micromeritics). Thermogravimetric experiments were run (Setsys from Setaram) in order to analyze the thermal stability of each sample after calcination, following a 5 K min^{-1} slope until 1073 K.

Temperature-programmed reduction experiments were carried out using a TPD/R/O-1100 instrument (ThermoFisher). Prior to the TPR run, the fresh sample was treated in a stream of argon (>99.999%, flowing at 20 mL min^{-1}), ramping the temperature at 10 K min^{-1} from RT to 573 K and maintaining it for 60 min, and then cooled to 313 K. The TPR measurement was carried out using H_2/Ar (4.98% v/v) as a reducing gas mixture, flowing at 20 mL min^{-1}, ramping the temperature at 5 K min^{-1} from RT to 1173 K and maintaining it for 20 min, and then cooled to 313 K.

Scanning electron microscopy (SEM) was performed using a JEOL JSM 5800LV (W filament). The samples were deposited onto carbon tape and treated by carbon sputtering. Energy-dispersive X-ray spectroscopy was performed with a diode Si–Li (PGT).

XPS analyses were performed at room temperature using an Axis Ultra^{DLD} (Kratos analytical) spectrometer with monochromatic and focused (analyzed zone of 300 × 700 μm^2, 150 W) Al Kα radiation (1486.6 eV) under a residual pressure of 5×10^{-9} mbar, with charge neutralization and deposition of powder samples on carbon tape. The hemispherical analyzer functioned at a constant pass energy of 160 eV for scanning and at 20 eV for quantitative analyses. The experimental bands were fitted to theoretical line shapes (70% Gaussian, 30% Lorentzian) using Shirley-type background subtraction. Quantitative analyses were performed using the appropriate atomic relative sensitivity factors (given by the constructor). Reference binding energy (BE) was C1s (284.6 eV, internal reference).

The microcalorimetric studies were performed using a Tian–Calvet heat-flow microcalorimeter (C80 from Setaram) at 353 K, coupled with a volumetric line providing precise pressure measurement (Barocel capacitance manometer) of the NH_3 and SO_2 gas probes used, respectively, for the analysis of acidic and basic sites. Sulfur dioxide (Air Liquide, purity > 99.999%) and ammonia (Air Liquide, purity > 99.995%) were used. A detailed description of the technique can be found elsewhere.[5,6] The samples were outgassed at 573 K for 12 h prior to each microcalorimetric measurement. The differential heats of adsorption were measured as a function of the coverage, by sending successive doses of the gas probe onto the sample until an equilibrium pressure of about 66 Pa was reached. Then the sample was evacuated for 30 min at the same temperature and a re-adsorption experiment was carried out in order to determine the chemisorption uptake (irreversibly adsorbed amount of probe, evaluated here at 26.7 Pa and 353 K).

Results and discussion

Influence of the preparation method on the acid–base properties of bulk oxides

Surface properties of the same compound can strongly vary with the particle size and the crystallinity.[15–17] As an example we displayed in Table 2 the evolution of acid–base features

Table 1 Precursors' molar ratios, effective molar ratios of metals in the calcined oxides and specific surface area (BET) of the different samples

	Precursors' molar ratios[a]		Effective[b] Zn : Me Me = Ga, Al or In	Surface area BET/m^2 g^{-1}
	Zn nitrate	Other nitrate		
ZnO "nit"	1	0	100 : 0	32
Commercial ZnO "com"			100 : 0	5
$Zn_3Ga_1O_x$	0.75	0.25	78 : 22	117
$ZnGaO_x$	0.5	0.5	53 : 47	118
Ga_2O_3 "nit"	0	1	0 : 100	134
Commercial Ga_2O_3 "com"			0 : 100	28
$Zn_3Al_1O_x$	0.75	0.25	74 : 26	130
$ZnAlO_x$	0.5	0.5	49 : 51	130
Al_2O_3 "nit"	0	1	0 : 100	420
Commercial Al_2O_3 "com"			0 : 100	115
$Zn_{19}In_1O_x$	0.95	0.05	96 : 4	37
$Zn_9In_1O_x$	0.9	0.1	91 : 19	57
$Zn_3In_1O_x$	0.75	0.25	78 : 22	41
$ZnInO_x$	0.5	0.5	55 : 45	55
In_2O_3 "nit"	0	1	0 : 100	46
Commercial In_2O_3 "com"			0 : 100	5

[a] Oxalic acid and urea were introduced in molar ratios of 1 and 2 respectively. [b] Determined by ICP-OES analysis.

Table 2 Specific surface area (SA), irreversibly adsorbed amounts of basic (NH_3) and acidic (SO_2) gas probes and crystallinity of zinc oxide samples

	SA[a]/m^2 g^{-1}	Cryst.[b]/nm	$V_{irrev}SO_2$	$V_{irrev}NH_3$
ZnO com	5	100	4.46	4.1
ZnO nano	11	50	4.32	1.4
ZnO nit	22	25	3.12	1.6

[a] BET analysis. [b] Evaluated by Scherrer's formula from XRD data.

among three bulk zinc oxide materials, a first commercial oxide ("com"), a second of nanometric size (~50 nm diameter) obtained by intensive milling ("nano") and a last one synthesized from the nitrate salt calcined at low temperature ("nit"). The commercial zinc oxide displays high amounts of both acidic and basic features well balanced, the more amorphous sample prepared from the nitrate salt displays twice more basic than acidic sites and the nanometric sample appears essentially basic, while the crystallinity and the specific surface area vary strongly among all samples. Thus when crystallinity and surface area vary, expected differences in acid–base properties are confirmed.

Then we investigated the differences of acid–base character between the synthesized bulk oxides (ZnO, Al_2O_3, Ga_2O_3, In_2O_3) and the commercial ones. The synthesized samples display an enhanced specific surface area (see Table 1) mainly due to the low temperature of calcination (673 K) compared to the commercial samples (above 1273 K for ZnO). The amounts of acidic and basic sites are significant enough to call them amphoteric, however the balance differs slightly from the commercial samples, often more crystalline. In order to compare their relative acid–base characters, we have displayed in Fig. 1 the irreversibly adsorbed volumes (chemisorption uptakes) for the NH_3 and the SO_2 gas probes corresponding, respectively, to a titration of the acidic and basic sites, without concern for their energy. As a complementary key we have reported in Fig. 2 the graphs of differential adsorption energy *vs.* the adsorbed amounts of gas probe, in order to observe the differences in strength of the acid–base sites for each bulk oxide. Fig. 2 displays how similarly amphoteric the bulk oxides are, with a slightly more enhanced basicity (left) for the synthesized ZnO, In_2O_3 and Al_2O_3, and a slightly more enhanced acidity (right) for the synthesized Ga_2O_3 and the commercial In_2O_3.

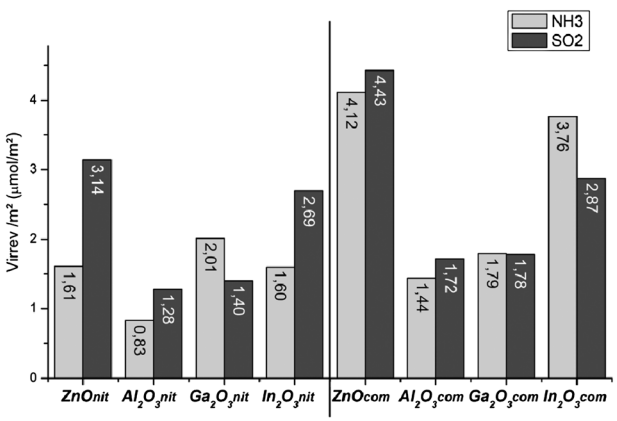

Fig. 1 Irreversibly adsorbed volumes of NH_3 and SO_2 for commercial samples and bulk oxides synthesized from nitrate salts.

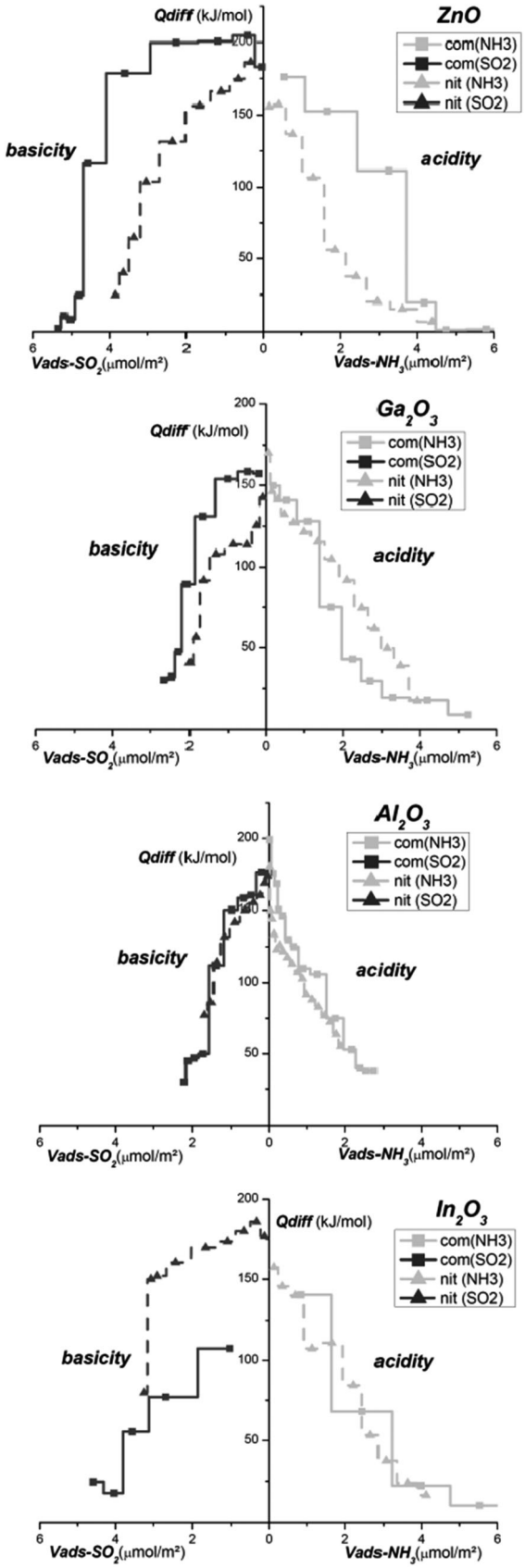

Fig. 2 Differential heats (kJ mol^{-1}) of SO_2 and NH_3 adsorption for each sample ("com" and "nit") of ZnO, Ga_2O_3, Al_2O_3 and In_2O_3.

Differential adsorption energy curves provide more information on the strength differences, such as the slightly more pronounced heterogeneity of the basic sites on synthesized ZnO (no clear plateau while the commercial sample displays a plateau around 200 kJ mol^{-1}), the highly enhanced strength of the basic sites on synthesized In_2O_3 "nit" (170 kJ mol^{-1}) compared to "com" (100 kJ mol^{-1}) and the slightly decreased strength of the basic sites of Ga_2O_3 "nit" (115 kJ mol^{-1}) compared to "com" (155 kJ mol^{-1}).

We observed a higher amount of acid sites per mass of catalyst on the "nit" than on the "com" ZnO sample (37 μmol g^{-1} instead of 20 μmol g^{-1}), but a lower amount per square metre of the catalyst's surface (1.6 μmol m^{-2} instead of 4.1 μmol m^{-2}), and a balance shifted towards basicity. Although the amount of acid sites remains far lower than the results presented by Naik and Fernandes (2–7 mmol g^{-1}),[2] these were obtained at higher temperature (~600 K) and with a TPD setup. The "acidity" value is not displayed at 353 K by Naik *et al.* but it can be estimated from the TPD derived "acidity" graph (value at 393 K and slope) at about 0.1 mmol g^{-1}, which is closer to the result we obtained.

Mixed oxides of zinc with Group 3 elements

Secondly, mixed oxides were prepared in order to develop amphoteric surfaces similar to zinc oxide but slightly differently shaped or with additional properties. Series with molar ratios Zn : Me of 75 : 25 and 50 : 50 (Me = Al or Ga or In) were compared to bulk oxides. The homogeneity of the calcined mixed oxides was checked with SEM and energy-dispersive X-ray spectroscopy, which measured proximity of both metal elements below the third of micrometre; Fig. 3 presents a SEM image of the $GaZnO_x$ sample where EDX was performed on the target, displaying relative amounts of both metals similar to bulk measurements by ICP-OES (Zn: 61 mol% by EDX instead of 53 by ICP-OES; Ga: 39 mol% instead of 47). X-Ray diffraction experiments revealed only bulk oxide crystallites and globally amorphous powders.

Fig. 4a displays the irreversibly adsorbed volumes ("V_{irrev}") of NH_3 and SO_2 gas probes on the series of Ga–Zn samples as well as the specific surface areas. Specific surface areas are

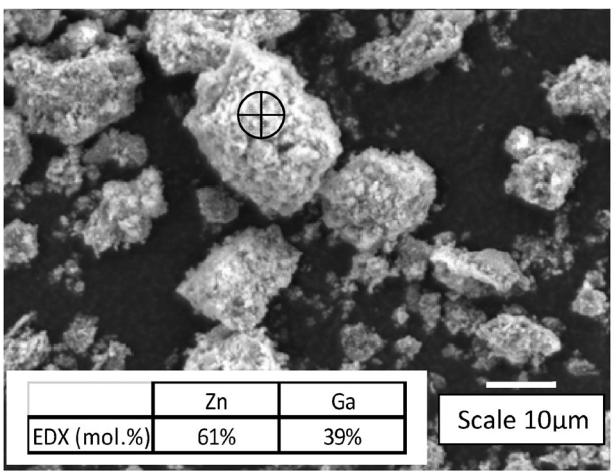

Fig. 3 SEM picture of GaZnOx (1 : 1) and target where relative amounts of metal Zn/Ga were evaluated by EDX (inserted table).

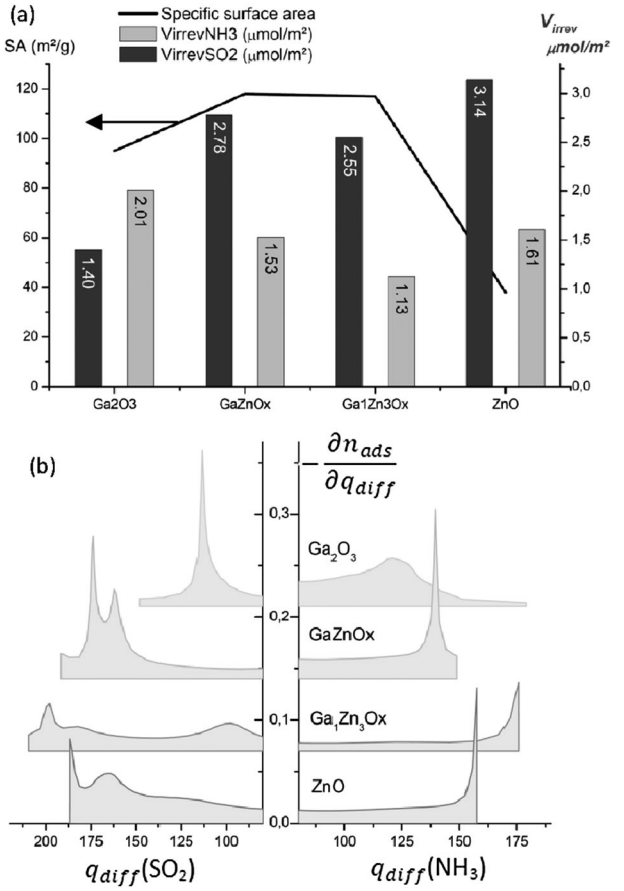

Fig. 4 (a) Irreversibly adsorbed amounts of NH_3 and SO_2 for the {1 : 0, 1 : 1, 1 : 3, 0 : 1} series of mixed oxides of gallium–zinc, and their corresponding specific surface areas (straight line). (b) Spectra of basicity (left) and acidity (right) for the same samples.

slightly increased (120 m^2 g^{-1}) and it can be observed how zinc–gallium mixed oxides display acid–base amounts and a ratio of acidic sites over basic sites similar to zinc oxide. By fitting the differential energy of adsorption (q_{diff} as a function of n_{ads}) and differentiating its inverse curve, we can plot an energy spectrum ($-\partial n_{ads}/\partial q_{diff}$ in μmol m^{-2}/(kJ mol^{-1}) as a function of q_{diff} in kJ mol^{-1}). The interaction of SO_2 or NH_3 with any surface will reach different scales of energy, due to their intrinsic properties (gas phase basicity or proton affinity for NH_3, oxygen affinity for SO_2...); with ammonia, strong interactions will reach 130 to 180 kJ mol^{-1} while physisorption would be considered below 80 kJ mol^{-1}, with sulfur dioxide, strong interactions will reach 150 to 210 kJ mol^{-1} while physisorption will be considered below 100 kJ mol^{-1}. Physisorption energies can be evaluated with the data collected during a re-adsorption experiment.

Fig. 4b features a spectrum of the energies of SO_2 and NH_3 adsorption for the Ga–Zn mixed oxide series, where it can be seen that the mixed oxides' acid strength (right) is profiled more like ZnO (clear peak corresponding to an energy plateau) and at higher energy than the gallium oxide main plateau. Besides, the basic strength's profile (left) also displays similarity between the two mixed oxides and ZnO (shape and high energy > 150 kJ mol^{-1}). Thus the impact of mixing zinc and gallium into an oxide does not appear to bring much more than shifts in energy, but it actually

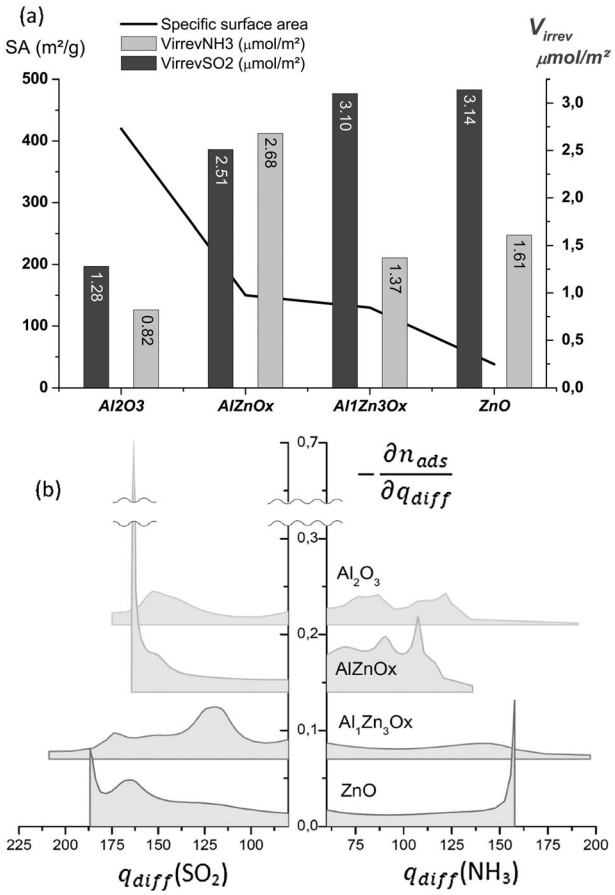

Fig. 5 (a) Irreversibly adsorbed amounts of NH_3 and SO_2 for the {1 : 0, 1 : 1, 1 : 3, 0 : 1} series of mixed oxides of aluminium–zinc, and their corresponding specific surface areas (straight line). (b) Spectra of basicity (left) and acidity (right) for the same samples.

provides solids of higher specific surface area than Ga_2O_3 and with the acid/base features of ZnO.

Concerning the series of Al–Zn mixed oxides, Fig. 5a displays their amounts of acidic ("$V_{irrev}NH_3$") and basic sites ("$V_{irrev}SO_2$"). While the specific surface area is found to decrease almost linearly with the aluminium content, the mixed oxides appear very differently shaped; the $AlZnO_x$ sample appears very similar to Al_2O_3 both in shape (ratio acid/base $\approx$ 1) and in amounts per gram of catalyst, while the $Al_1Zn_3O_x$ sample appears almost identical to ZnO in its shape (ratio acid/base $\approx$ 2) and amounts per surface of catalyst. Besides, when considering the evolution of amounts with decreasing aluminium content, it appears that $AlZnO_x$ displays additional acid sites apparently unrelated to the parent bulk oxides. The energy spectra of SO_2 and NH_3 adsorption displayed in Fig. 5b confirm the similarity of Al_2O_3 and $AlZnO_x$ (basicity around 150–160 kJ mol^{-1} and very heterogeneous and medium to weak acidity), while $Al_1Zn_3O_x$ displays a plateau mainly for medium basic strength (120 kJ mol^{-1}) quite lower than ZnO (170 kJ mol^{-1}) and a less pronounced acidity peak. To summarize, with similar acid/base amounts ZnO and $Al_1Zn_3O_x$ display very different acid/base strength populations, while Al_2O_3 and $AlZnO_x$ appear similar in energy shape but not in amounts, and the "non-linearity" of $AlZnO_x$'s total acidity ("$V_{irrev}NH_3$") corresponds to medium to weak acid strengths.

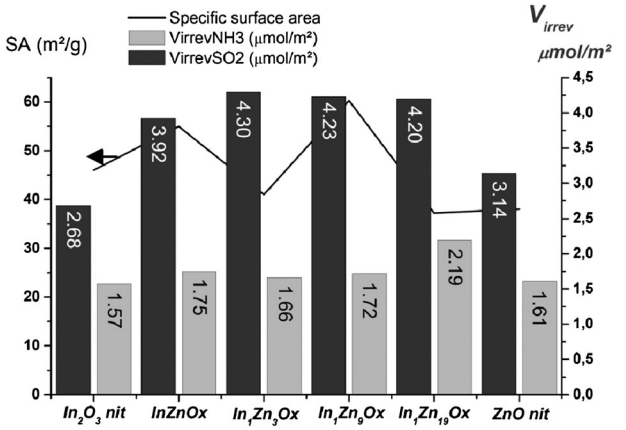

Fig. 6 Irreversibly adsorbed amounts of SO_2 and NH_3 gas probes and specific surface area for the In–Zn series.

Special interest was brought on the indium–zinc series, because of the seemingly increasing basicity with decreasing indium loading observed on the 50 : 50 and 75 : 25 samples, and because of the redox properties of indium(III) oxide that can be of interest for the dehydration/dehydrogenation competition. Additionally mixed oxides of Zn : In molar ratio 90 : 10 and 95 : 5 were then prepared (resulting in 91 : 9 and 96 : 4, respectively, see Table 1) and were also analyzed by adsorption microcalorimetry. Fig. 6 reports the irreversibly adsorbed volumes of SO_2 and NH_3 for samples of the In–Zn series, as well as their specific surface areas, which appear stable around 45 m^2 g^{-1}. While the irreversibly adsorbed volume of NH_3 is stable around 1.6 μmol m^{-2}, the volume of SO_2 is higher by 1–1.5 μmol m^{-2} for the mixed oxides than for the parent bulk oxides. The amount of basic sites corresponding to the adsorption of SO_2 remains similar with decreasing indium content, indicating that the supplementary basicity does need only the low presence of indium in the zinc oxide matrix to be effective.

Fig. 7 displays the spectra of SO_2 adsorption for the In–Zn series, where a shift in strength can be observed for the mixed oxides, both in initial differential energy (180 kJ mol^{-1} for the bulk oxides and 200–235 kJ mol^{-1} for the mixed oxides) and in the energies of the plateaus. The increased basicity of these mixed oxides then corresponds also to a shift in strength and not to supplementary basic sites besides the In_2O_3 and ZnO sites.

Temperature programmed reduction (TPR) was carried out on the series of In–Zn samples in case a redox feature could affect the adsorption of sulfur dioxide, however no critical shift in the onset temperature (about 723 K for a 5 K min^{-1} slope) of the indium reduction peak could be observed and the onset of zinc oxide reduction did not appear before 1250 K. For every sample the amount of H_2 consumption was fitted at 1.4 molar equivalent (0.996 correlation coefficient), corresponding to 2.8 degree of oxidation, attributed to indium species which is coherent with its presumed +III oxidized state (In_2O_3). Then it is improbable that indium may play a redox role in the presence of these basic features.

When descending the Group 3 column, mixed oxides with zinc display enhanced acidity (Al–Zn), then the usually balanced features (Ga–Zn) and finally enhanced basicity (In–Zn), following a slight evolution in electronegativity

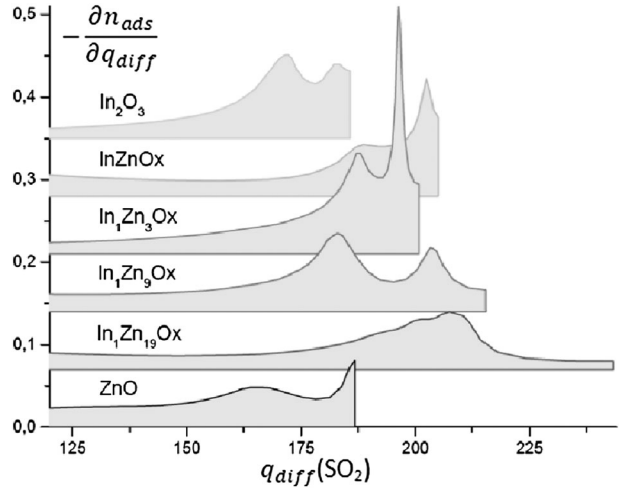

Fig. 7 Energy spectrum of SO_2 adsorption for the In–Zn series zoomed on the [120, 240 kJ mol^{-1}] section.

(from 1.61 to 1.81 to 1.78 in the Pauling scale) and an increase in effective ionic radius (from 53.5 to 80 pm). The very similarity of $Al_1Zn_3O_x$, $GaZnO_x$ and $Ga_1Zn_3O_x$ with ZnO in terms of both total amounts and strengths of acidic/basic sites can be explained with a possible migration of zinc atoms towards the surface and gallium/aluminium towards the core, such as explained by theory.[18] Such an effect is dependent on the differences in effective atomic radii (53.5 and 62 pm for Al^{3+} and Ga^{3+}, respectively, and 74 pm for Zn^{2+}), thus stronger for Al–Zn than for Ga–Zn, and predicting a surface mainly influenced by ZnO properties, such as observed in our case. The migration effect regarding In–Zn mixed oxides should appear in a less extent (indium effective ionic radius = 0.80 Å) and in the opposite way, then it would be less relevant in a series of low indium content. The surface abundances of In and Zn measured by X-ray photoelectron spectroscopy confirm this tendency of indium to migrate towards the surface, until 3.3 times higher abundance on the surface than in the bulk for the 96 : 4 sample (Fig. 8), however in our case the apparition of enhanced basicity does not correlate directly with indium content or migration.

It has been shown that at 353 K the interaction of ZnO with SO_2 only involves the surface oxygens[19] and that the formed SO_3 species do not decompose before 400 K, however above 473 K phenomena of ZnO reduction have been observed on SO_2 adsorbed samples.[20] The presence of indium in the system could affect the interaction of ZnO with SO_2. XPS analyses on the O1s peaks of the In–Zn series reveal three peaks at 529.2, 530.0 and 531.1 eV assigned, respectively, to O^{2-} (bound to In^{3+}), O^{2-} (bound to Zn^{2+}), and oxygen-deficient regions.[21] Peaks related to O–In and O–Zn are quantitatively coherent with the amounts of metal elements. Besides, the relative amount of the oxygen-deficient regions' peak evolves similarly to the basicity measured by adsorption microcalorimetry (Fig. 9), however high binding energy oxygen regions are not likely to be responsible for enhanced basicity.

When comparing with the deconvolution of the commercial ZnO's O1s peak, similar features are obtained. It has to be reminded that in Fig. 2, ZnO "com" displays high basic strength (plateau at 200 kJ mol^{-1}) in an important amount

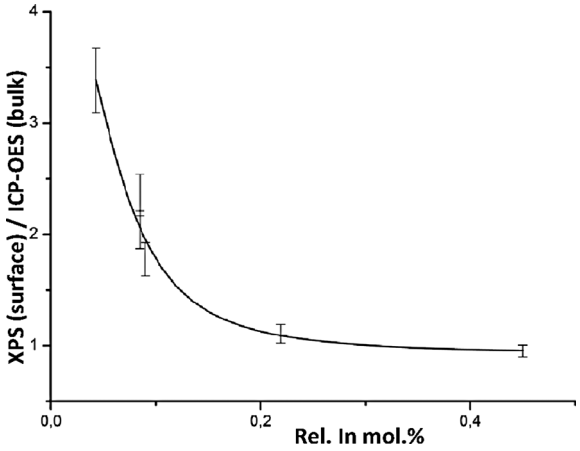

Fig. 8 Relative abundance of indium on the surface, plotted as the ratio of relative indium molar percentages (In/(In + Zn)) with XPS and ICP-OES.

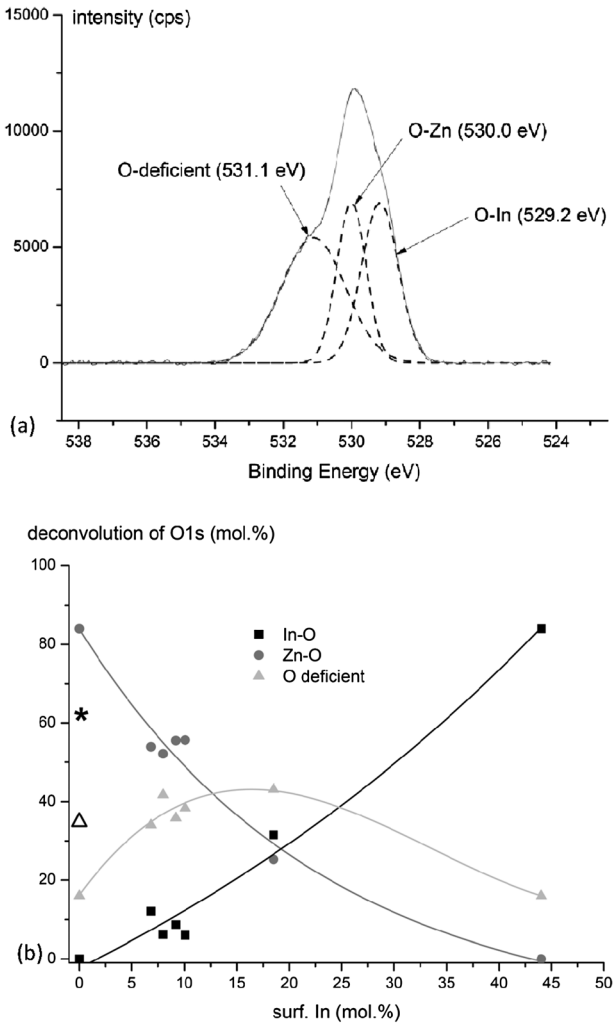

Fig. 9 (a) XPS spectrum of $InZnO_x$'s O1s, deconvoluted into O^{2-} bound to In^{3+} (In–O), to Zn^{2+} (Zn–O) and oxygens of O-deficient regions and (b) deconvolution of XPS O1s peaks of the In–Zn series, as a function of the surface molar ratio of indium, and of the commercial ZnO ("★" for In–O, "Δ" for O-deficient).

($3.10\ \mu mol\ m^{-2}$ of sites of adsorption energy above $170\ kJ\ mol^{-1}$), both similar to In–Zn mixed oxides. The surface oxygens responsible for strong basic features could originate from the ZnO structure only and would be more pronounced in materials of higher crystallinity. The In–Zn mixed oxide series would then be able to stabilize these surface features, eventually ZnO crystallites, more than the pure oxides prepared with the same process. XRD could not distinguish the surface from core crystallites and the In–Zn series was of overall low crystallinity. Another explanation may be the *n*-doping of indium(III) inside the zinc(II) oxide matrix that could provide additional electrons for the reaction with sulfur dioxide, however this phenomenon could not explain the features of the $InZnO_x$ sample. Acid sites of In–Zn mixed oxides, besides, remain very similar to the pure oxides synthesized from nitrate. Actually Kung's and Tanabe's models are in agreement with the absence of additional acid sites in such mixed oxides.[22,23]

Thus, with In–Zn mixed oxides, it was possible to reproduce crystalline ZnO's basicity while improving the specific surface area considerably, and besides acidity was kept relatively low. This type of mixed oxide will find its application in dehydration or dehydrogenation catalysis such as the conversion of carboxylic acids (formic acid to fatty acids), and the oxygen vacancies on the surface of the catalyst[24] as well as the redox features can have an important effect on selectivity. Besides it has to be noted that this series of catalysts displays important basic features of high strength (q_{diff} (SO_2 ads.) $> 200\ kJ\ mol^{-1}_{SO_2}$) in substantial amounts ($1-2\ \mu mol\ m^{-2}_{catalyst}$), whose impact on efficiency or selectivity of catalytic dehydration/dehydrogenation can be valuable.

Conclusions

Series of binary oxides of zinc and elements from Group 3 (Al, Ga, In) displaying amphoteric character were synthesized using an intimate solid mixture process adapted from Naik *et al.* and analyzed with adsorption microcalorimetry, providing solids of good homogeneity, enhanced specific surface area and important acid–base features. The Al–Zn mixed oxides display enhanced amounts of medium and weak acid sites whereas the In–Zn mixed oxides display enhanced amounts of highly basic sites, which remain even at low indium content. While their specific surface area is ten times higher, their basicity is similar in amount per surface area and strength with the commercial and more crystalline ZnO, whereas their acidity remains lower, similar to that of synthesized bulk oxides. Series of amphoteric oxides are pertinent for the catalytic dehydrogenation and dehydration phenomena, for they can provide variable amounts and strengths of basic and acidic sites, and they can provide as well solids of similar acid–base character but with additional physico-chemical properties (redox, oxygen vacancies, porosity, crystallinity...).

Acknowledgements

The authors are thankful to the scientific services of IRCELYON. The research leading to these results has received funding from the European Union Seventh Framework Programme (FP7/2007-2013) under grant agreement no. 241718 EuroBioRef.

Notes and references

1 K. Tanabe and W. F. Hölderich, *Appl. Catal., A*, 1999, **181**, 399–434.
2 S. P. Naik and J. B. Fernandes, *Thermochim. Acta*, 1999, **332**, 21–25.
3 A. L. Petre, J. A. Perdigon-Melon, A. Gervasini and A. Auroux, *Catal. Today*, 2003, **78**, 377–386.
4 A. Gervasini and A. Auroux, *J. Therm. Anal.*, 1991, **37**, 1737–1744.
5 A. Auroux, *Top. Catal.*, 1997, **4**, 71–89.
6 S. Bennici and A. Auroux, *Thermal analysis and calorimetric method*, in *Metal oxide catalysis*, ed. S. D. Jackson and J. S. Hargreaves, Wiley-VCH, Verlag GmbH & Co, 2009, 391–442.
7 A. Gervasini and A. Auroux, *J. Phys. Chem.*, 1990, **94**, 6371–6379.
8 B. Gergely, A. Rédey, C. Guimon, A. Gervasini and A. Auroux, *J. Therm. Anal. Calorim.*, 1999, **56**, 1233–1241.
9 J. A. Perdigon-Melon, A. Gervasini and A. Auroux, *J. Catal.*, 2005, **234**, 421–430.
10 Z. R Tian, J. A. Voigt, J. Liu, B. Mckenzie, M. J. Mcdermott, M. A. Rodriguez, H. Konishi and H. Xu, *Nat. Mater.*, 2003, **2**(12), 821–826.
11 G. Eranna, B. C. Joshi, D. P. Runthala and R. P. Gupta, *Crit. Rev. Solid State Mater. Sci.*, 2004, **29**, 111–188.
12 J. Strunk, K. Kahler, X. Xia and M. Muhler, *Surf. Sci.*, 2009, **603**, 776–1783.
13 S. Mahmud, M. J. Abdullah, G. Putrus, J. Chong and A. K. Mohamad, *Synth. React. Inorg. Met.-Org. Chem.*, 2006, **36**, 155.
14 S. P. Naik and J. B. Fernandes, *Appl. Catal., A*, 2001, **205**, 195–199.
15 O. W. Perez-Lopez, A. C. Farias, N. R. Marcilio and J. M. C. Bueno, *Mater. Res. Bull.*, 2005, **40**, 2089–2099.
16 A. Baiker and J. Kijenski, *Catal. Rev.*, 1985, **27**(4), 653.
17 S. P. Naik and J. B. Fernandes, *Stud. Surf. Sci. Catal.*, 1998, **113**, 513–517(Recent Advances in Basic and Applied Aspects of Industrial Catalysis).
18 S. Y. Liu and H. H. Kung, *Surf. Sci.*, 1981, **110**, 504–522.
19 J. A. Rodriguez, T. Jirsak, S. Chaturvedi and M. Kuhn, *Surf. Sci.*, 1992, **442**, 400–412.
20 A. R. Gonzalez-Elipe and J. Soria, *Z. Phys. Chem. (München, Ger.)*, 1982, **132**(1), 67–74.
21 W. Kim, J.-H. Bang, H.-S. Uhm, S.-H. Lee and J.-S. Park, *Thin Solid Films*, 2010, **519**, 1573–1577.
22 H. H. Kung, *J. Solid State Chem.*, 1984, **52**, 191–196.
23 K. Tanabe, T. Sumiyoshi, K. Shibata, T. Kiyoura and J. Kitagawa, *Bull. Chem. Soc. Jpn.*, 1974, **47**(5), 1064–1066.
24 M. Aizawa, Y. Morikawa, Y. Namai, H. Morikawa and Y. Iwasawa, *J. Phys. Chem. B*, 2005, **109**, 18831–18838.